Research Square

Preprints are preliminary reports that have not undergone peer review.
They should not be considered conclusive, used to inform clinical practice,
or referenced by the media as validated information.

A Computational Intelligence Framework for Data-Driven Shape Optimization Using GRA and GA-BPNN

Qingchun Wu
Kunming University of Science and Technology
Weilin Liu
1572544887@qq.com
Kunming University of Science and Technology
Nanyi Wang
Beijing Institute of Technology

Research Article

Keywords: Purple Clay Teapot, KE, GRA, GA-BPNN

Posted Date: November 5th, 2026

DOI: https://doi.org/10.21203/rs.3.rs-11102473/v1

License: This work is licensed under a Creative Commons Attribution 4.0 International License.
Read Full License

Additional Declarations: No competing interests reported.

A Computational Intelligence Framework for Data-Driven Shape Optimization Using GRA and GA-BPNN

Qingchun Wu[1], Weilin Liu[2], Nanyi Wang[3]
[1]Kunming University of Science and Technology, Kunming, 650031 China
[2]Kunming University of Science and Technology, Kunming, 650031 China
[3]Beijing Institute of Technology, Beijing, 100081, China

Corresponding author: Welin Liu (1572544887@qq.com).

ABSTRACT Traditional product shape optimization suffers from single-objective tuning, low prediction precision, and inefficient nonlinear mapping between design variables and performance. To address the limitations of conventional Backpropagation Neural Network (BPNN), such as weak optimization ability and low prediction accuracy in shape design, this paper proposes an intelligent optimization framework integrating Grey Relational Analysis (GRA) and Genetic Algorithm-optimized BPNN (GA-BPNN) for purple clay teapot shape design. First, a standardized teapot shape database is established, and morphological decomposition and factor analysis are performed to extract and screen key shape parameters. GRA is then applied to quantify correlations between parameters and objective dimensions, determining four core inputs for the neural network. On this basis, GA is used to optimize the initial weights and thresholds of BPNN, overcoming slow convergence and local optima issues. The GA-BPNN model achieves accurate nonlinear mapping from subjective design requirements to three-dimensional shape parameters and outputs the globally optimal shape combination. Experimental results and user tests show that the optimized scheme exhibits superior objective matching and user satisfaction, with significantly higher prediction accuracy and convergence efficiency than the standard BPNN. This work establishes a complete intelligent optimization workflow for product shape design, which supports high-precision multi-parameter optimization and nonlinear function mapping. The proposed hybrid method has strong scalability and can be extended to general shape optimization and multi-parameter decision-making tasks, providing a data-driven approach for intelligent design applications.

INDEX TERMS Purple Clay Teapot; KE; GRA; GA-BPNN

I. INTRODUCTION

The purple clay teapot, made from unique Yixing clay, has a 500-year history dating back to the late Ming Dynasty and is universally recognized as the best tea brewing vessel (Young and Yixing 2016)[1]. The purple clay teapot embodies profound cultural significance, carrying the essence of traditional Chinese culture and national art (Chen 2014)[2], and compared with porcelain, it has excellent breathability and is less prone to deformation (Xian and Won 2017)[3]. With technological innovations and changes in consumer concepts, studies of purple clay teapot design lack element associations. This research constructs a quantitative mapping model, breaks traditional frameworks and provides a foundation for building a scientific theoretical system. In research on purple clay teapots and their shapes, Yong (2010)[4] discussed the image design, facial expressions, and connotations of purple clay teapots. Feng (2019)[5] analyzed the semantic meaning of purple clay teapot shapes from the perspective of Wu culture and traditional imagery, deriving the concept of harmonious creation. Zhang et al. (2013)[6] applied reverse engineering technology to manufacture molds for purple clay teapots. Most research on purple clay teapots focuses only on shaping techniques and craftsmanship (Fan et al. 2008)[7]; traditional cultural spirit (Luo 2016)[8]; decorative techniques (Xie and Lin 2018)[9]; the physical properties of clay materials (Fan et al. 2010)[10]; and the impact of different clays on tea quality (Li et al. 2021)[11]. The existing research lacks a systematic analysis of the associations between user emotional imagery and design elements, leading to problems in the Purple Clay Teapot

market and industry. This research constructs a framework to address these gaps, with KE providing support.

Intelligent algorithm models (IAM) integrate technologies such as artificial intelligence (AI) and machine learning and can autonomously learn, adaptively optimize, and solve complex problems. Li et al. (2018)[12] reviewed the research prospects of intelligent algorithms in optimizing complex systems and intelligent modeling. Mnih et al. (2015)[13] verified the robustness of intelligent algorithms in handling complex tasks. Gong et al. (2020)[14] addressed the shortcomings of traditional data-driven models in terms of interpretability and knowledge fusion, showing that IAM, driven by core knowledge, simulates human intelligence to handle complex environmental tasks efficiently. An increasing number of scholars are applying IAM in various fields, such as education, where Wang N et al. (2024)[15] constructed intelligent algorithm models to enhance prediction performance, whereas Zhang et al. (2025)[16] proposed the YOLO CP intelligent monitoring algorithm. In the medical field, Shen et al. (2009)[17] combined rough sets with probabilistic neural networks to construct an intelligent diagnostic system for heart disease. De-Kun et al. (2022)[18] designed a new mobile intelligent evaluation algorithm in the sports field. With the continuous development of AI, more scholars are beginning to study the application of IAM in design. Wang N et al. (2024)[19] proposed the SSA-LSTM-Attention model for intelligent cockpit design in new energy vehicles. Zhao et al. (2013)[20] studied control algorithms for the smooth operation of electromagnetically guided intelligent vehicles. Zhou et al. (2003)[21] integrated multiple technologies and developed virtual systems with the help of intelligent algorithms. Using intelligent algorithms, Li and Zhao (2020)[22] optimized models on the basis of aircraft assembly perception data. Gong and Gao (2024)[23] proposed a home design method that combines virtual reality with intelligent algorithms. However, no scholars have explored the application of intelligent algorithms in purple clay teapots. IAM can help precisely capture needs and optimize features, but it struggles with capturing implicit emotions and making humanized decisions and value judgments. Therefore, it is necessary to introduce emotional design methods into the development of purple clay teapot shapes.

As a rapidly developing discipline, KE studies new design concepts to capture innovation (Zhou 2011)[24]; at the same time, it is a new product development technology based on consumer-oriented theory (Peng 2008)[25]. KE has six key characteristics: logicality (Jeong 2003)[26], integration (Uemura et al. 1999)[27], emotionality (Kang et al. 2025)[28], experimentalism, data-driven nature (Lai et al. 2006)[29], and reliability (Marco-Almagro and Tort-Martorell 2012)[30]. At the same time, the KE aims to convert customer emotions into design (Su et al. 2007)[31]. As more scholars have applied KE theory in the design field (Table 1), Bu et al. (2019)[32] applied quantitative theory-based affective imagery methods to study the shape of ceramic teapots. Liu and Ieee (2020)[33] established a linear regression model between the morphological elements of palace lanterns and affective imagery. Wang and Wang (2018)[34] applied KE to explore the modeling needs of elderly people for home service robots. Duan et al. (2022)[35] applied KE and quantitative theory I (QTI) to increase the design efficiency of textile machinery models. Ren X et al. (2025)[36] combined the StyleGAN model for style generation with particle swarm optimization support vector regression (PSO-SVR) to build a mapping model for social robot form and user perception.

TABLE I
RESEARCH SUBJECTS, METHODS, OBJECTIVES, AND CONTENT RELATED TO THE KE

Reference	Research Object	Research Method	Research Objective	Main Content
Bu et al. (2019)	Ceramic Teapot	Based on quantitative theory, an image mapping model is constructed using focus groups and questionnaires.	Explore the form and styling of ceramic teapots to provide a basis for their design and evaluation.	Based on quantitative theory, an image mapping model is constructed using focus groups and questionnaires.
Liu and Ieee (2020)	Palace lantern	Extracting elements from sensory engineering and constructing mathematical models through the SD method and statistical analysis.	Analyze the form of palace lanterns, construct element and image regression models to empower design.	Extract vocabulary elements from palace lantern samples and use the SD method to model and verify design associations.
Wang and Wang (2018)	The styling needs of older adults for home service robots.	Based on intuitive engineering, establish a semantic database for denoising and quantitative analysis.	Exploring the needs and importance of design elements for home service robots among the elderly population.	Analyze sensory cognition of sample modeling, extract main factors, clarify imagery-element mapping, design & verify

				method.
Duan et al. (2022)	The styling design of textile machinery	Select sample word pairs based on sensory engineering and QTI to build a correlation model.	Satisfy users' sensory needs for textile machinery styling and improve design efficiency.	Determine the sample word pairs for the drawing machine, model the solution strategy, and validate the model.
Ren X et al. (2025)	Social robots for public health interventi on	Combining StyleGAN with PSO-SVR and other methods.	To enhance the attractivene ss of social robots and explore the combinatio n of AIGC and KE.	Generate new samples, deconstruct features, and construct mapping models.

In previous KE studies, Kuang and Jiang (2009)[37]reported that excessive reliance on sample databases could solidify user emotions and shape feature mappings, leading to the homogenization of product shape semantics. Guo et al. (2016)[38] studied the mapping of mobile phone design variables and user emotional imagery through the BPNN intelligent algorithm model, utilizing GA global search to optimize parameters and generate solutions that align with emotional preferences. Experiments have validated its advantages in terms of multiobjective balance and breaking homogenization while enhancing innovation capabilities. Many successful GA-BPNN models have been developed, such as those by Zhang et al. (2021)[39], who developed a combination of ultrasound technology and the GA-BPNN model. Sun et al. (2023)[40] used the GA-BPNN model to predict the roughness of drainage pipes containing silt. Hu and He (2016)[41] proposed the GA-BPNN intrusion detection algorithm.

This paper, under the IMA and KE research frameworks, uses the GA-BPNN composite intelligent algorithm model to learn the existing purple clay teapot shapes on the market and ultimately generate new purple clay teapot shapes, creating a new purple clay teapot shape sample database that aligns with user emotional needs. The structure and content of the remaining paper are as follows: Chapter 2 introduces the relevant research methods. Chapter 3 presents the purple clay teapot shape design research framework and conducts design validation. Chapter 4 discusses the research content. Chapter 5 summarizes the main contributions of this paper and the current research limitations.

II. RESEARCH METHODS

A. Factor Analysis (FA)

FA is a multivariate statistical method based on dimensionality reduction that is used for preliminary analysis in empirical research (Young and Hong 2007)[42] and is applied in various fields, such as social sciences (Liu et al. 2016)[43], medicine and health (Mainous and 3rd 1993)[44], education (Sun and Hyung-Ryong 2013)[45], and finance (YU and LIU 2022)[46]. Its goal is to reduce many original variables into a smaller set of new composite factors while minimizing information loss (Mainous and 3rd, 1993)[44]. In product shape design, FA, in combination with KE, is used to study the association of users' subjective intention vocabulary and classify it accurately. For example, Chen et al. (2021)[47] used affective vocabulary selection, the SD to collect evaluations, and factor analysis to associate design elements. Jing et al. (2024)[48] constructed a furniture emotional imagery factor library through word selection, experimentation, and factor analysis. On the basis of KE, Su et al. (2011)[49] used the fuzzy analytic hierarchy process and FA to construct a material imagery model.

The FA standardizes the mean data of emotional vocabulary during the algorithm operation to eliminate dimensionality; the applicability is tested through the KMO test (KMO) and Bartlett's sphericity test (BOST). where *rij* is the simple correlation coefficient between variables *i* and *j* and where *aij* is the partial correlation coefficient between variables *i* and *j*. The KMO formula is as follows:

$$KMO = \frac{\sum_{i \neq j} r_{ij}^2}{\sum_{i \neq j} r_{ij}^2 + \sum_{i \neq j} a_{ij}^2} \tag{1}$$

where *n* is the sample size, *p* is the number of variables, $|R|$ is the determinant of the correlation matrix *R*, and the BTOS formula is as follows:

$$x^2 = -\left[n - 1 - \frac{2_p + 5}{6}\right] \cdot ln|R| \tag{2}$$

The correlation matrix is calculated on the basis of standardized data, and the principal component method is used to extract the factor loading matrix. Orthogonal rotation is then applied to form an easily interpretable component matrix. In the rotated component matrix, *A* is the factor loading matrix before rotation ($p \times m$, where p is the number of variables and where m is the number of common factors); *T* is the orthogonal rotation matrix ($m \times m$, satisfying TTT=I). ; *A* is the rotated loading matrix, where element *aij* represents the correlation between variable *i* and factor *j*. The larger the absolute value is, the more significant the variable's contribution to the factor. The orthogonal rotation formula is as follows:

$$A = A \cdot T \tag{3}$$

Finally, the principal component score coefficient matrix (PCSC) transforms variables into factor scores, reducing dimensionality and providing a lower-dimensional space for subsequent analysis. Let the score coefficient of the *k-th* principal component be wik, where $i=1,2,...,p$; $k=1,2,...,m$; p_{ik}

is the *i-th* element of the eigenvector corresponding to the *k-th* principal component; λ_k is the eigenvalue of the *k-th* principal component; and F_k is the principal component score, where z_i is the standardized variable. The PCSC formula is as follows:

$$w_{ik} = \frac{p_{ik}}{\sqrt{\lambda_k}} \tag{4}$$

$$F_k = \sum_{i=1}^{p} w_{ik} \cdot z_i \tag{5}$$

As data development has advanced toward efficient high-dimensional data processing, incorporating this into purple clay teapot design can improve data processing efficiency and support precise design.

B. GRAY RELATIONAL ANALYSIS (GRA)

Chinese scholars pioneered gray system theory, a new interdisciplinary field widely applied in various domains (Xie and Chen 2019)[50]. The core of GRA is to compare the dynamic trends of data sequences and quantify the influence of factors on the main behavior of the system, with a higher correlation indicating a greater influence. The GRA is applied in fields such as economics, psychology, and design. For example, Fujun et al. (2010)[51] validated the effectiveness of data envelopment analysis-weighted GRA in the Yangtze River Delta. YANG et al. (2023)[52] reported that photovoltaic prediction via GRA is similar, and AdaBoost outperforms a convolutional neural network (CNN). Li et al. (2018)[53] integrated GRA with entropy weighting methods to build a model. Dong et al. (2020)[54] proposed a risk assessment model for Pb-Zn mines via fuzzy gray relational analysis. Xu et al. (2016)[55] used GRA to predict car shape evolution trends and verified the method. Zhang et al. (2023)[56] used shape grammar and GRA to model and validate the feasibility of the SC200 elevator. Xue and Yi (2019)[57] used GRA to study the seat shape and color design of high-speed trains.

In the GAR model, the feature and mother sequences are first processed to be dimensionless by normalizing the values to eliminate dimensionality effects. Each sample value of the *k-th* element in each sequence ($k = 1, 2,...,h$) is processed, where *Ci(k)* is the *k-th* sample value of the feature sequence *Ci; Ci* is the mean of the feature sequence *Ci; E(k)* is the *k-th* sample value of the mother sequence *E*; and *E* is the mean of the mother sequence *E*. The normalization formula is as follows:

$$\mathrm{C_i'(k)} = \frac{\mathrm{C_i(k)}}{\overline{\mathrm{C_i}}}, \mathrm{E'(k)} = \frac{\mathrm{E(k)}}{\overline{\mathrm{E}}} \tag{6}$$

Next, the difference between the mother sequence and each feature sequence at each sample point is calculated, where *Δik* is the difference between feature sequence *Ci* and mother sequence *E* at the *k-th* sample point. Then, the global minimum and maximum differences among all absolute differences are determined, where min(min) represents the minimum absolute difference between all feature sequences and the mother sequence across all sample points and where max(max) represents the maximum absolute difference between all feature sequences and the mother sequence across all sample points. The formula for calculating the absolute difference sequence is as follows:

$$\Delta_i(k) = \left|E'(k) - C_i'(k)\right| \tag{7}$$

The formula for the global minimum and maximum differences is as follows:

$$\begin{aligned} min\,min &= min_i\, min_k \Delta_i(k), \\ max\,max &= max_i\, max_k \Delta_i(k) \end{aligned} \tag{8}$$

The discrimination coefficient (discrimination coefficient $\rho = 0.5$) is then used to calculate the correlation coefficient for each sample point to reflect the degree of local correlation, where *ξik* is the correlation coefficient between feature sequence *Ci* and mother sequence *E* at the *k-th* sample point. The formula for calculating the correlation coefficient is as follows:

$$\xi_i(k) = \frac{min\,min + \rho \cdot max\,max}{\Delta_i(k) + \rho \cdot max\,max} \tag{9}$$

The overall correlation degree is obtained by averaging the correlation coefficients of each feature sequence, and the results are ranked, realizing a quantitative analysis of the correlation degree between features and the mother sequence. *γi* is the overall correlation degree between feature sequence *Ci* and mother sequence *E*, and *s* is the number of feature correlation degrees. The formula for calculating the degree of correlation is as follows:

$$\gamma_i = \frac{1}{n}\sum_{k=1}^{n} \xi_i(k) \tag{10}$$

The correlation degrees of the *s* features are arranged in descending order, with larger correlation degrees indicating a more significant impact of the feature on the core factor of emotional imagery. Therefore, based on KE theory, this paper uses GRA to analyze the degree of correlation between feature sequences and the mother sequence, selecting morphology features with high degrees of correlation. The formulas for arranging in descending order are as follows:

$$\gamma sort = [\gamma_{i1}, \gamma_{i2}, \dots, \gamma_{is}],\ \ \gamma_{i1} \geq \gamma_{i2} \geq \cdots \geq \gamma_{is} \tag{11}$$

C. GENETIC ALGORITHM–OPTIMIZED BACKPROPAGATION NEURAL NETWORK (GA-BPNN)

(1) BACKPROPAGATION NEURAL NETWORK (BPNN)

The BPNN is a supervised learning algorithm that outputs through forward propagation, calculates errors, and updates weights through backpropagation. It introduces nonlinearity via the activation function, making the predictions approach real values. Du et al. (2021)[58] used a BPNN to determine the parameters of an internet credit warning model. Liu et al. (2006)[59] combined ant colony optimization with a BPNN to develop a hybrid neural network. Sun et al. (2017)[60] used BPNN convolutional pooling to extract features. Sang (2021)[61] combined a BPNN and a support vector machine (SVM) GA to assess credit risk in supply chain finance

applications. Ding et al. (2023)[62] constructed a color evaluation model based on BPNN latent measurements for electric irons. Guo et al. (2016)[63] used a BPNN and a GA to optimize web page experience. Therefore, this paper uses a BPNN to establish a nonlinear mapping relationship between the highest correlated key morphological features of purple clay teapot and the core imagery dimension factors. The algorithm model is constructed as shown in Figure 1.

The input data are standardized, where x is the original data, μ is the feature mean, and σ is the feature standard deviation. The formula is as follows:

$$x_{norm} = \frac{x - \mu}{\sigma} \tag{12}$$

The sigmoid function is used in the hidden layer to normalize the mapping of the shape parameters. This function maps the input values to the (0, 1) range, introducing nonlinearity into the neural network. The formula is as follows:

$$\sigma_{(z)} = \frac{1}{1 + e^{-z}} \tag{13}$$

In forward propagation, the signals from the input layer are passed through the weights and biases to the hidden layer, processed by the ReLU function, and then passed to the output layer to obtain the predicted values. Here, the output of the hidden layer is h, and the prediction from the output layer is y. W_1 represents the weights from the input layer to the hidden layer, W_2 represents the weights from the hidden layer to the output layer, and b_1 and b_2 are the biases.

Backpropagation uses the mean squared error (MSE) as the loss function, where N is the number of samples, y_i is the true value, and $\hat{y}_i$ is the predicted value. The formula is as follows:

$$h = \sigma(W_1 \cdot X_{train} + b_1) \tag{14}$$

$$\hat{y} = W_2 \cdot h + b_2 \tag{15}$$

$$MSE = \frac{1}{N}\sum_{i=1}^{n}(y_i - \hat{y}_i)^2 \tag{16}$$

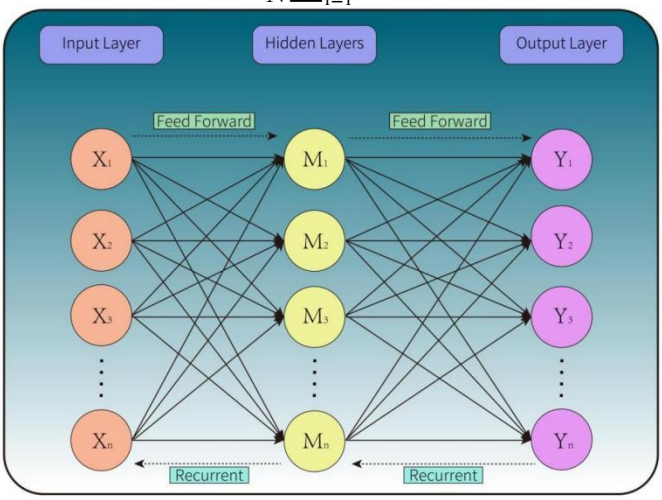


FIGURE 1. Neural Network Structure Model

(2) GENETIC ALGORITHM (GA)

The GA is a global optimization algorithm that simulates the biological evolution process and iteratively searches for the optimal solution to a problem through selection, crossover, and mutation operations. Civilian and Daewonkim (2015)[64] describe the GA as a search algorithm that iteratively uses population and genetic operators (selection, crossover, mutation). The selection strategy influences convergence and divergence, and the algorithm avoids local optima by optimizing solutions on the basis of individual performance, making it suitable for complex problems. GA is widely applied in various fields. For example, Azuma et al. (2009)[65] used a GA to obtain haplotype frequencies from genotype frequencies; Shi (2020)[66] researched the application of a GA in the optimization design of large building structures; Son et al. (2021)[67] used a GA to improve asymmetric encryption algorithms and intermediate information transmission layers; Yu (2008)[68] proposed an image restoration method based on a GA; Diego-Mas et al. (2016)[69] developed a model based on a GA and neural networks to predict users' judgments of the environmental friendliness of different tables. Tian (2008)[70] optimized an ANN via a GA and fuzzy theory to solve the complex mapping problem between car transmissions and internal combustion engines. Therefore, this paper uses a BPNN to construct a nonlinear mapping between purple clay teapot shape features and imagery factors and utilizes a GA to optimize parameters, generating target imagery design solutions. The process is shown in Figure 2.

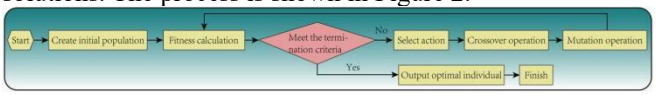


FIGURE 2. GA flowchart

The performance of the BPNN model's test set is used as the basis for fitness evaluation, with the mean squared error (MSE) as the fitness function, where $y_{test,i}$ is the true value of the test set and $\hat{y}_{test,i}$ is the predicted value of the test set. The formula is as follows:

$$Fitness = \frac{1}{N}\sum_{i=1}^{N}(y_{test,i} - \hat{y}_{test,i})^2 \tag{17}$$

The roulette wheel selection method is used to select superior individuals from the current population for reproduction, with each individual's selection probability P_i, where M is the population size. Moreover, the arithmetic crossover method (formula 19) is used, where p_1 and p_2 are the parent chromosomes and where α is the crossover coefficient. A random value between 0 and 1 is chosen. The new individual mutation operation uses the Gaussian mutation method (formula 20), where ci is the gene value, σ is the mutation step size, and $N(0,1)$ is the standard normal distribution. Therefore, this study first uses the BPNN model to construct a nonlinear mapping model between product emotional imagery and morphological features. The GA model is subsequently used for continuous iterative optimization of this model.

$$P_i = \frac{Fitness_i}{\sum_{j=1}^{M} Fitness_j} \tag{18}$$

$$c_1 = \alpha \cdot p_1 + (1 - \alpha) \cdot p_2 \;;\; c_2 = (1 - \alpha) \cdot p_1 + \alpha \cdot p_2 \tag{19}$$

$$c_i' = c_i + \sigma \cdot N \tag{20}$$

III. RESEARCH PROCESS AND RESULTS

A. METHODS

This study addresses the issue of the missing correlation between user emotional imagery and morphological features in traditional purple clay teapot design by constructing an "imagery analysis-feature association-algorithm generation" data quantification framework. First, 80 typical samples are selected by experts to build the database, followed by the collection of 100 emotional vocabulary words through questionnaires. Using the Kawakita-Jiro method for classification, 18 representative words were obtained. The SD collects ratings from 103 users, and the FA extracts the four core imagery dimensions. Morphological analysis was subsequently used to deconstruct eight categories and 69 morphological elements. The GRA is applied to establish a quantitative mapping, and four core features with a correlation of ≥0.70 are selected. The GA-BPNN model is subsequently constructed, and after 2800 generations of evolution, it achieves nonlinear conversion from emotional language to 18 morphological parameters. This study overcomes traditional limitations, establishing a quantitative research paradigm and providing a complete methodological system. It holds significant value for digitalizing intangible cultural heritage and integrating cultural heritage with AI. The research framework is shown in Figure 3. The experimental procedures were approved by the Medical Ethics Committee of Kunming University of Science and Technology, and the relevant guidelines and regulations were followed. Informed consent was obtained from all participants.

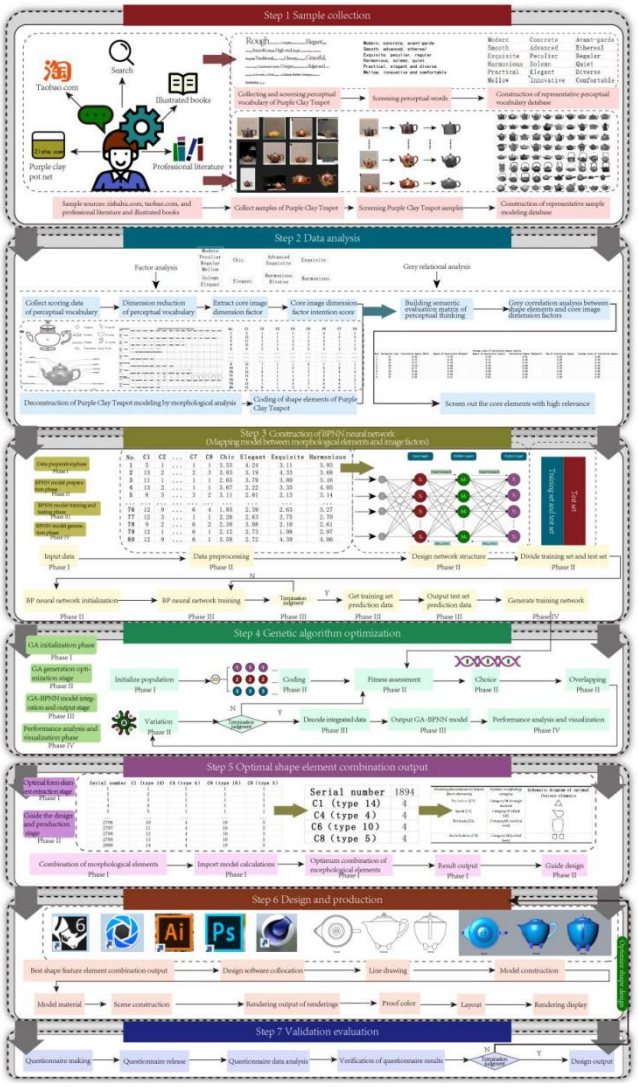


FIGURE 3. Research Framework

B. CONSTRUCTION OF PURPLE CLAY TEAPOT SHAPE IMAGERY DATA AND DIMENSION ANALYSIS

(1) SAMPLE COLLECTION

This study collected 398 samples from the Purple Clay Teapot website, Taobao, professional literature, and catalog books, covering six major teapot shapes, to establish a sample database. The goal is to provide rich and typical foundational materials for subsequent analysis of purple clay teapot shapes and aesthetic feature summaries. The sample images must display the overall shape and detailed features of the purple clay teapot without issues such as blurry double images, distortion, or chaotic backgrounds while ensuring diversity and comprehensiveness in the representation of shape styles. Blurry and cluttered images were removed to prevent visual fatigue from excessive samples that could interfere with participants' evaluations when selecting the Purple Clay Teapot sample database. After evaluation and selection by experts and scholars, 80 purple clay teapots were chosen as representative samples on the basis of shape classification.

Additionally, Photoshop was used to apply grayscale processing to the samples to avoid color influence, thereby building the purple clay teapot sample database (Figure 4).

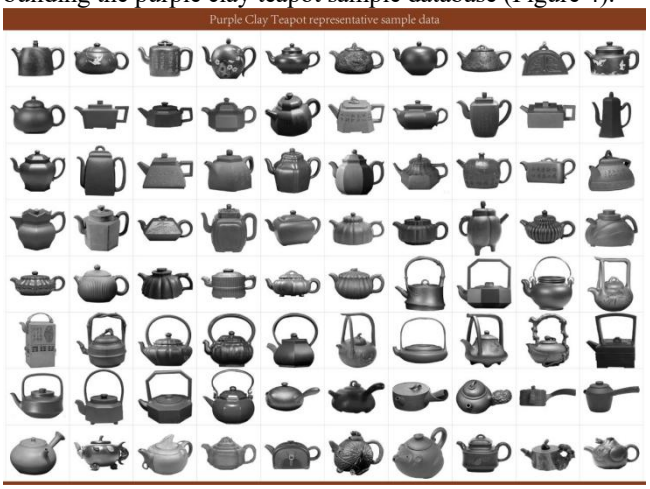


FIGURE 4. Sample Database

(2) EMOTIONAL VOCABULARY COLLECTION

The users' initial emotional intentions regarding purple clay teapot shapes were collected through a questionnaire. The initial survey included 15 experts, 20 designers, 40 design students, and 25 members of the general public; 100 emotional vocabulary words were collected. These were then narrowed down to 18 by 40 design scholars. Scores were subsequently collected for the 18 vocabulary words and 80 representative samples from 13 experts，as shown in Table II, 80 design students, and 20 public members via a 7-point rating scale (Figure 5).

TABLE II
18 EMOTIONAL VOCABULARY WORDS

Modern	Figurative	Pioneering	Smooth	High-end	Ethereal
Exquisite	Unique	Neat	Harmonious	Majestic	Serene
Solid	Elegant	Diverse	Rounded	Innovative	Comfortable

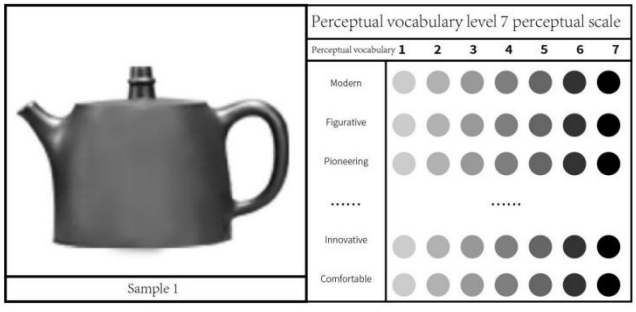


FIGURE 5. 7-Level Emotional Vocabulary Scale

(3) IMAGERY DATA DIMENSION ANALYSIS

The FA is used to reduce the dimensionality of the emotional vocabulary; 10 vocabulary words from the 18 are selected, Table III, a total of 103 valid questionnaires were collected, and the average values were calculated, as shown in Table IV. and the score matrix data are imported into SPSS for processing. The KMO and Bartlett tests were performed, with a KMO value of 0.707, indicating good overlap of variable information, making it suitable for factor analysis. Bartlett's test of sphericity showed a significance of 0.000 (<0.05), rejecting the hypothesis of variable independence and indicating significant correlations between variables, as shown in Table V. In Figure 6, the vocabulary is scattered in three-dimensional space with no obvious clustering, reflecting the differences in loadings on the component representative dimensions and illustrating the multidimensional distinctions of imagery.

TABLE III
10 EMOTIONAL VOCABULARY WORDS

Modern-B1	High-end-B2	Exquisite-B3	Unique-B4	Neat-B5
Harmonious-B6	Majestic-B7	Elegant-B8	Diverse-B9	Rounded-B10

TABLE IV
EMOTIONAL VOCABULARY RATING DATA

NO	B1	B2	B3	B4	B5	B6	B7	B8	B9	B10
1	3.52	3.08	3.13	3.87	3.37	3.59	3.55	4.93	4.27	3.34
2	3.88	4.64	4.02	4.31	4.89	3.97	3.21	3.17	3.39	2.25
3	3.92	3.7	3.9	2.31	1.96	2.77	4.39	3.19	3.55	2.4
4	4.1	3.07	3.62	3.27	2.99	4.71	2.45	1.98	3.38	4.3
5	2.87	2.64	1.62	3.37	2.1	2.46	2.26	1.76	3.81	4.1
6	3.28	2.71	2.76	2.32	3.08	2.64	1.39	3.27	3.68	4.5
7	3.01	2.85	3.83	4.81	3.59	5.85	4.04	3.56	3.59	4.29
8	3.53	3.38	3.19	5.08	4.9	1.62	3.82	5.01	4.45	5.05
9	4.61	2.49	2.2	4.63	4.26	1.57	3.05	4.6	4.46	4.67
10	3.63	3.35	3.04	2.42	3.49	3.24	4.13	3.54	3.45	3.37
11	3.36	4.2	2.92	5.24	2.47	3.76	4.03	3.44	3.48	2.7
12	4.04	3.16	4.3	4.34	3.4	4.54	2.4	3.7	3.43	2.52
13	3.49	3.54	3.2	4.59	3.27	5.22	2.2	3.61	3.34	3.29
14	1.92	3.05	4.78	3.02	3.1	2.68	1.87	2.16	3.15	3.72
15	2.17	2.46	2.94	2.94	4.56	2.79	2.23	1.71	3.29	4.34
16	2.49	1.61	1.88	2.11	3.85	4.6	3.21	3.7	4.37	4.74
17	4.61	2.1	2.84	3.46	4.17	3.43	3.31	4.78	3.51	4.85
18	3.49	2.91	3.31	3.77	4.99	2.6	2.78	3.26	3.48	4.63
19	2.78	2.59	3.28	3.96	3.58	4.49	4.1	3.4	3.47	4.02
20	2.96	3.6	4.29	4.07	2.04	2.25	4.37	3.44	3.53	4.24
21	2.98	3.62	3.5	3.03	3.15	4.69	3.78	3.27	3.67	4.03
22	3.7	3.68	4.66	3.02	2.06	3.93	2.18	1.71	4.21	4.03
23	3.85	3.43	3.55	2.93	3.85	3.66	2.27	1.47	3.96	3.96
24	3.71	4.38	2.42	2.86	3.16	2.94	1.94	3.51	4.09	3.91
25	5.15	4.57	4.38	5.45	3.36	3.26	3.88	4.93	4.44	4.93
26	4.37	1.78	3.86	4.39	2.83	3.82	4.45	3.11	4.35	4.57
27	2.96	3.39	1.11	3.68	3.24	4.66	3.76	0.92	3.36	3.69
28	3.59	3.01	2.48	2.84	5.11	1.51	2.21	2.14	2.97	3.41
29	2.92	3.02	2.13	4.15	4.99	2.35	2.13	3.18	2.88	3.51
30	2.84	2.58	3.02	4.62	2.83	4.97	2.32	2.92	3.09	3.51
31	3.77	3.06	2.86	2.97	3.43	3.37	3.46	3.31	3	3.34
32	4.6	2.64	5.13	5.7	2.18	5.31	5.07	4.19	2.98	4.12
33	4.52	5.44	5.62	3.53	5.73	2.8	4.84	3.93	3.52	3.73
34	3.68	2.98	2.98	4.16	2.67	3.43	3.49	3.02	3.73	3.69
35	3.63	4.88	3.92	4.34	3.82	4.26	4.48	1.68	3.31	3.83
36	3.62	3.15	2.14	2.53	2.55	2.41	2.52	2.13	3.54	2.99
37	2.55	2.39	2.18	2.42	4.31	5.44	2.87	2.12	3.64	3
38	2.58	2.12	4.17	3.31	3.26	3.22	2.9	3.42	3.85	2.9
39	2.7	3.17	4.72	5.13	4.32	3.27	3.11	3.34	3.68	3.38
40	4.67	5.21	5.46	4.46	5.35	4.84	4.72	3.92	3.27	4.1
41	4.66	5.61	5.8	2.96	3.86	5.12	3.87	4.05	3.3	3.83
42	3.5	3.49	2.24	4.75	4.27	4.01	5.29	2.76	3.31	2.41
43	3.88	4.7	3.78	3.48	2.97	3.69	3.25	3.83	4.28	2.74
44	2.25	3.71	3.55	2.85	1.52	2.75	3.21	3.05	4.37	2.1
45	2.68	2.33	4.73	2.7	3.08	1.28	2.06	1.89	4.48	2.72
46	2.63	1.59	2.4	2.54	4.34	4.54	1.88	2.08	3.97	4.55
47	3.22	1.53	3.57	4.44	1.43	3.96	2.93	2.1	2.84	4.11
48	3.82	4.75	4.93	3.53	4.26	5.81	1.3	3.26	2.94	4.29
49	4.29	3.81	4.55	4.93	3.78	4.62	3.35	3.09	2.67	3.52
50	2.33	1.32	2.94	2.26	2.34	2.09	1.97	5	2.76	4.49
51	2.56	2.5	3.81	2.15	1.52	3.31	1.89	3.49	2.98	4.33
52	2.59	1.42	2.66	3.15	2.24	2.39	3.96	3.67	3.03	4.29
53	2.55	3.48	2.83	3.38	1.17	2.48	4.09	3.85	4.5	4.51
54	1.86	2.72	3.52	4.35	3.78	5.81	3.42	4.28	4.11	4.01
55	2.02	2.7	3.46	2.76	3.82	1.61	1.53	4.06	4.07	3.01

56	3.63	1.86	5.03	4.04	5.26	4.28	2.25	2.32	4.07	3.29
57	3.46	4.94	4.59	3.55	2.73	3.8	2.56	2.35	3.96	3.46
58	1.79	3.83	2.71	2.13	1.99	4.3	3.25	3.78	4.33	3.25
59	1.96	4.02	3.07	2.1	3.63	1.62	1.25	3.64	4.21	3.51
60	2.05	3.54	2.72	1.29	1.5	4.47	1.09	4.03	3.84	2.31
61	1.83	3.69	3.45	1.06	0.12	1.54	4.16	3.56	2.49	2.19
62	1.27	3.08	2.78	2.33	2.03	2.93	3.22	3.7	2.56	3.16
63	1.44	1.38	4.81	2.18	2.03	3.77	4.13	3.44	2.35	3.36
64	4.23	1.61	5.82	4.55	4.01	3.67	2.21	2.19	2.57	3.05
65	3.48	4.01	4.09	3.45	3.03	3.86	2.28	2.34	2.6	2.29
66	1.58	3.68	2.32	4.08	4.55	5.88	1.02	1.37	2.57	2.91
67	1.81	3.78	4.31	1.56	3.5	1.26	1.25	1.42	2.67	2.97
68	2.67	3.7	2.14	4.4	2.32	2.81	3.84	1.42	2.61	3.29
69	2.58	1.97	2.35	2.04	4.29	3.88	4.19	1.37	3.86	3.04
70	2.49	2.2	4.4	2.14	2.21	2.37	3.92	1.58	4.25	2.26
71	1.51	2.32	3.01	1.24	3.21	2.36	1.39	1.32	4.02	1.98
72	3.82	5.71	2.13	3.92	4.42	3.95	2.51	2.34	3.94	2.63
73	3.72	4.41	2.74	3.86	3.94	3.91	2.16	2.49	3.08	2.32
74	2.08	3.25	1.72	1.81	1.34	2.74	1.15	3.33	2.99	2.84
75	2.27	3.41	3.71	3.98	4.95	1.32	1.73	3.31	3.47	2.7
76	1.49	3.32	1.94	1.69	1.08	2.79	1.23	3.55	3.74	3.12
77	1.59	1.81	3.69	1.73	3.12	1.51	1.46	3.8	3.88	2.59
78	2.04	1.84	2.35	2.07	3.06	1.7	2.87	3.29	3.52	2.33
79	1.76	2.04	1.91	2.06	2.26	2.5	2.13	3.32	3.43	2.41
80	3.77	4.02	4.76	3.72	4.34	4.63	3.24	2.19	3.48	2.5

TABLE V
KMO AND BARTLETT'S TEST

KMO and Bartlett inspection		
KMO sampling suitability quantity		.707
Bartlett test	sphericity	Approximate chi square 141.225
		Freedom 45
		Significance .000

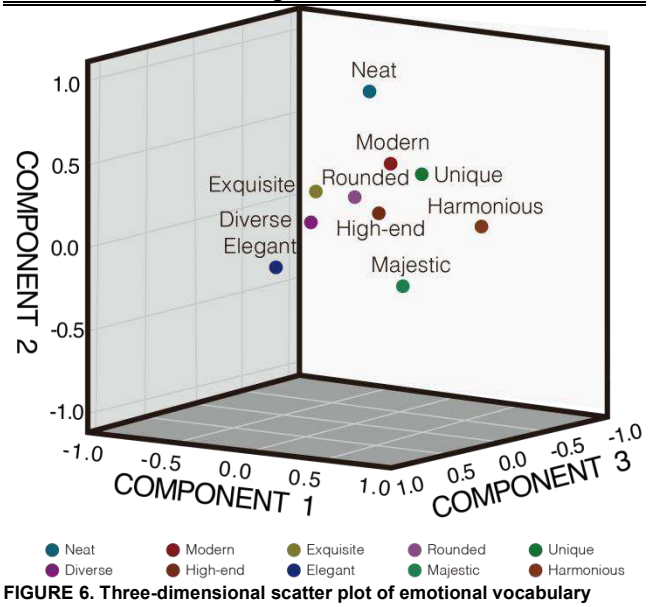


FIGURE 6. Three-dimensional scatter plot of emotional vocabulary

The Kaiser normalization maximum variance method is applied to perform orthogonal rotation on the emotional vocabulary score matrix, processing factors with absolute values <0.5, resulting in four high-loading variables, as shown in Table VI. Principal component analysis revealed four factors: the first group, "Modern, Unique, Neat, Rounded," formed the Chic factor; the second group, "Majestic, Elegant," formed the Elegant factor; the third group, "High-end, Exquisite," formed the Exquisite factor; and the fourth group, "Harmonious, Diverse," formed the Harmonious factor, corresponding to the four CIFs: Chic, Elegant, Exquisite, and Harmonious,as shown in Table VII. The component score coefficient matrix (Figure 7) provides the computational basis for quantitative design optimization. Combined with user classification and prototype testing, this approach can enhance the effectiveness of conveying purple clay teapot shape imagery.

TABLE VI
ROTATED COMPONENT MATRIX

Rotated component matrix[a]				
	Component			
	1	2	3	4
Modern	0.685			
High-end			0.821	
Exquisite			0.543	
Unique	0.726			
Neat	0.761			
Harmonious				-0.522
Majestic		0.702		
Elegant		0.704		
Diverse				0.812
Rounded	0.536			

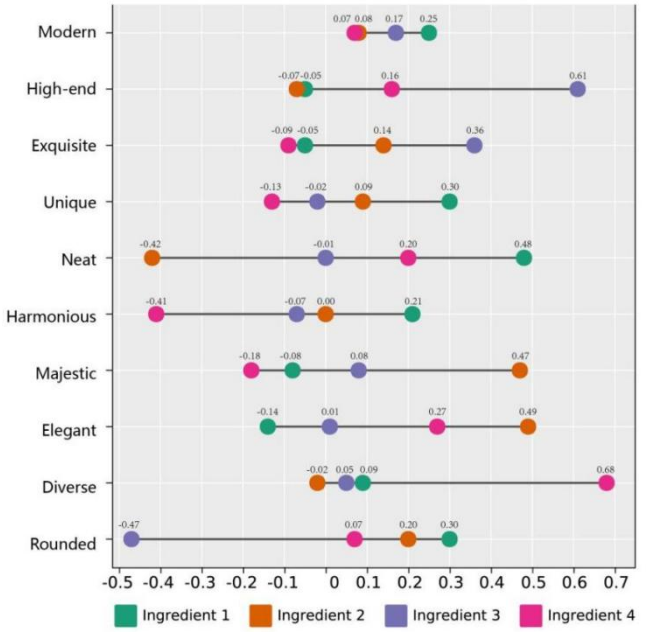


FIGURE 7. Principal component score coefficient matrix

TABLE VII
PRINCIPAL COMPONENT ANALYSIS REVEALED FACTORS

Ingredient1	Chic	**Ingredient3**	Exquisite
Ingredient2	Elegant	**Ingredient4**	Harmonious

C. EMOTIONAL EVALUATION MATRIX OF PURPLE CLAY TEAPOTS AND GRAY RELATIONAL ANALYSIS

(1) MORPHOLOGICAL FEATURE CONSTRUCTION

On the basis of the 80 collected representative purple clay-shaped samples, morphological decomposition breaks down the teapot shapes (Figure 8), dividing them into various morphological components. The component characteristics of purple clay teapots are decomposed into eight categories and

69 key morphological elements, simplifying the purple clay teapot shape decomposition factors, as shown in Figure 9.

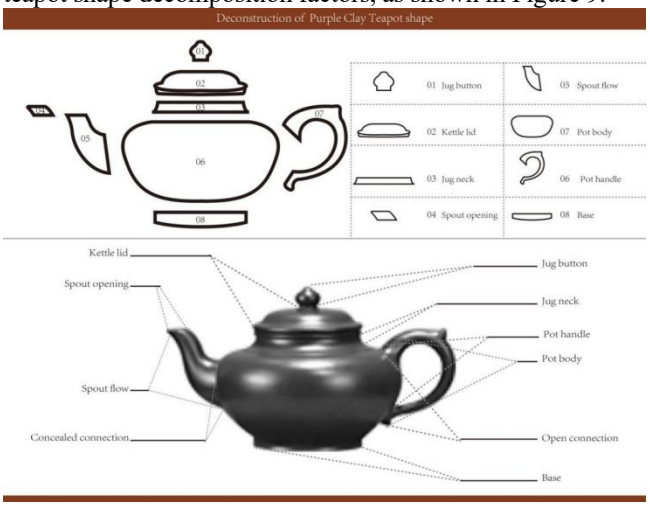


FIGURE 8. Shape decomposition diagram

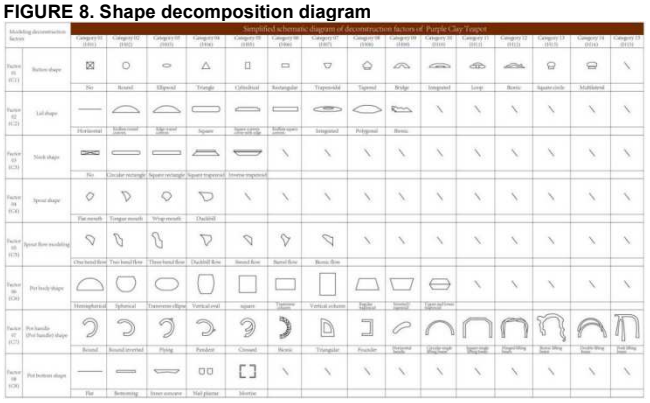


FIGURE 9. Diagram showing the simplification of shape decomposition factors

(2) CONSTRUCTION OF THE EMOTIONAL THINKING SEMANTIC EVALUATION MATRIX

After FA, 4 CIFs were obtained. A questionnaire survey was conducted with 10 experts, 45 graduate and undergraduate design students, and 15 members of the general public. They evaluated the core imagery dimension factors for 80 representative purple clay teapot samples. The scoring method used a 7-point Likert scale (1 = very dissatisfied, 7 = very satisfied). Seventy valid questionnaires were collected, and the average values were calculated. Using eight categories and 69 key morphological elements as the standard, 1--15 categories of parametric coding were sequentially applied to the 80 representative samples. The 8 key morphological elements are C1, C2, C3, C4, C5, C6, C7, and C8. Specifically, C1 contains 14 morphological elements with parametric coding from 1--14; C2 has nine elements, coded from 1--9; C3 contains five elements, coded from 1--5; C4 has four elements, coded from 1--4; C5 has seven elements, coded from 1--7; C6 has 10 elements, coded from 1--10; C7 contains 15 elements, coded from 1--15; and C8 contains five elements, coded from 1--5. The emotional thinking semantic evaluation matrix is shown in Table VIII.

TABLE VIII

EMOTIONAL THINKING SEMANTIC EVALUATION MATRIX

No	C1	C2	C3	C4	C5	C6	C7	C8	Chic	Elegant	Exquisite	Harmonious
1	5	1	1	1	1	5	1	1	3.53	4.24	3.11	3.93
2	13	2	1	1	1	3	2	3	3.83	3.19	4.33	3.68
3	11	1	1	3	3	5	1	1	2.65	3.79	3.80	3.16
4	13	2	1	2	3	2	1	1	3.67	2.22	3.35	4.05
5	8	3	4	2	2	3	3	2	3.11	2.01	2.13	3.14
6	12	9	1	3	1	3	2	1	3.30	2.33	2.74	3.16
7	13	1	1	3	2	2	1	1	3.93	3.80	3.34	4.72
8	9	9	1	1	6	8	1	1	4.64	4.42	3.29	3.04
9	13	1	1	1	6	1	1	1	4.54	3.83	2.35	3.02
10	6	3	4	1	6	6	1	1	3.23	3.84	3.20	3.35
11	13	2	2	3	1	3	1	2	3.44	3.74	3.56	3.62
12	6	6	3	3	1	9	8	4	3.58	3.05	3.73	3.99
13	14	8	5	2	5	6	8	2	3.66	2.91	3.37	4.28
14	14	2	5	3	1	6	1	2	2.94	2.02	3.92	2.92
15	7	8	5	3	6	6	1	1	3.50	1.97	2.70	3.04
16	12	4	5	3	5	8	8	4	3.30	3.46	1.75	4.49
17	14	5	4	3	1	3	1	2	4.27	4.05	2.47	3.47
18	14	6	3	1	2	4	1	1	4.22	3.02	3.11	3.04
19	6	6	2	1	5	6	8	1	3.59	3.75	2.94	3.98
20	14	2	1	1	3	7	1	1	3.33	3.91	3.95	2.89
21	13	8	1	3	3	7	3	1	3.30	3.53	3.56	4.18
22	9	2	1	3	3	7	3	1	3.20	1.95	4.17	4.07
23	14	6	1	1	5	8	8	1	3.65	1.87	3.49	3.81
24	6	8	1	3	1	8	1	1	3.41	2.73	3.40	3.52
25	14	8	1	3	3	7	1	1	4.72	4.41	4.48	3.85

26	14	3	1	3	2	5	3	1	4.04	3.78	2.82	4.09
27	14	8	1	1	5	6	3	1	3.39	2.34	2.25	4.01
28	14	1	1	1	6	2	3	1	3.74	2.18	2.75	2.24
29	12	2	1	3	1	6	4	1	3.89	2.66	2.58	2.62
30	4	2	3	3	1	8	7	1	3.45	2.62	2.80	4.03
31	13	1	3	4	4	4	3	1	3.38	3.39	2.96	3.19
32	13	6	2	3	3	5	1	1	4.15	4.63	3.89	4.15
33	9	1	1	3	2	10	1	1	4.38	4.39	5.53	3.16
34	6	6	3	3	3	7	1	4	3.55	3.26	2.98	3.58
35	13	3	3	3	2	6	1	1	3.91	3.08	4.40	3.79
36	14	8	1	3	1	6	3	1	2.92	2.33	2.65	2.98
37	14	1	2	3	1	3	1	2	3.07	2.50	2.29	4.54
38	13	2	3	1	6	5	1	4	3.01	3.16	3.15	3.54
39	13	8	2	3	1	3	4	2	3.88	3.23	3.95	3.48
40	6	1	2	3	1	8	3	4	4.65	4.32	5.34	4.06
41	14	8	1	1	1	3	1	1	3.83	3.96	5.71	4.21
42	14	2	1	3	1	6	1	1	3.73	4.03	2.87	3.66
43	13	1	2	3	1	6	3	1	3.27	3.54	4.24	3.99
44	14	9	1	3	3	6	6	4	2.18	3.13	3.63	3.56
45	9	8	3	1	2	3	1	4	2.80	1.98	3.53	2.88
46	12	2	1	3	1	3	3	1	3.52	1.98	2.00	4.26
47	9	1	1	1	5	6	10	1	3.30	2.52	2.55	3.40
48	6	5	4	1	3	5	11	1	3.98	2.28	4.84	4.38
49	1	7	4	3	3	10	10	2	4.13	3.22	4.18	3.65
50	9	2	3	3	1	6	15	1	2.86	3.49	2.13	2.43
51	1	1	1	3	3	7	14	1	2.64	2.69	3.16	3.15
52	12	2	1	3	3	6	12	2	3.07	3.82	2.04	2.71
53	14	8	4	1	3	10	10	2	2.90	3.97	3.16	3.49
54	13	8	4	3	2	9	10	2	3.50	3.85	3.12	4.96
55	13	1	3	3	1	8	10	2	2.90	2.80	3.08	2.84
56	12	8	1	3	1	1	15	1	4.06	2.29	3.45	4.18
57	10	7	2	1	5	1	10	1	3.30	2.46	4.77	3.88
58	13	2	1	3	1	8	15	4	2.29	3.52	3.27	4.32
59	12	2	1	3	2	6	13	4	2.80	2.45	3.55	2.92
60	14	2	1	3	5	6	11	5	1.79	2.56	3.13	4.16
61	14	7	2	3	2	6	10	1	1.30	3.86	3.57	2.02
62	14	7	2	3	3	9	10	4	2.20	3.46	2.93	2.75
63	14	2	1	3	1	9	11	1	2.25	3.79	3.10	3.06
64	2	3	5	2	5	6	10	1	3.96	2.20	3.72	3.12
65	13	2	1	1	6	3	9	1	3.06	2.31	4.05	3.23
66	11	2	1	3	1	8	9	4	3.28	1.20	3.00	4.23
67	12	1	1	1	6	6	9	1	2.46	1.34	4.05	1.97
68	11	3	1	1	6	10	9	1	3.17	2.63	2.92	2.71
69	12	2	1	2	3	6	9	1	2.99	2.78	2.16	3.87
70	3	2	1	1	6	9	9	1	2.28	2.75	3.30	3.31
71	13	1	1	3	6	10	9	1	1.99	1.36	2.67	3.19
72	12	2	1	3	7	9	6	4	3.70	2.43	3.92	3.95
73	12	2	1	3	1	2	5	1	3.46	2.33	3.58	3.50
74	9	2	1	3	1	6	6	2	2.02	2.24	2.49	2.87
75	6	1	1	3	1	6	6	1	3.48	2.52	3.56	2.40
76	12	9	1	1	7	2	6	4	1.85	2.39	2.63	3.27
77	12	3	1	1	7	2	1	1	2.26	2.63	2.75	2.70
78	9	2	1	3	1	6	6	2	2.38	3.08	2.10	2.61
79	12	1	1	3	7	6	6	1	2.12	2.73	1.98	2.97

80	12	9	1	3	1	6	6	1	3.58	2.72	4.39	4.06

(3) GRAY RELATIONAL VISUAL ANALYSIS

Four CIFs were used as the mother sequence, and eight key morphological elements were used as the feature sequence, with a discrimination coefficient of 0.5. Univariate analysis revealed that the highest correlation item under each imagery dimension was C1, with the second-highest item varying by dimension (Figure 10), reflecting differences in morphological feature preferences. In the comprehensive analysis, C1 has the highest total correlation of 3.20 and an average of 0.80. C6 (3.05/0.76), C4 (3.03/0.76), and C8 (2.81/0.70) show outstanding overall correlation levels and were selected as key morphological elements, as shown in Figure 11. The associations between features and imagery are clarified through quantitative methods, and core variables are selected to support model optimization and quantitative research.

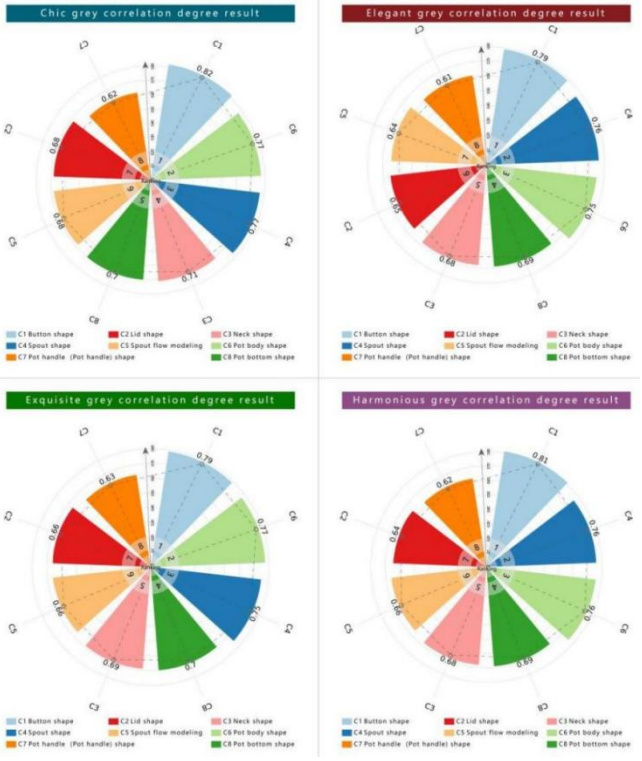


FIGURE 10. Gray Relational Results

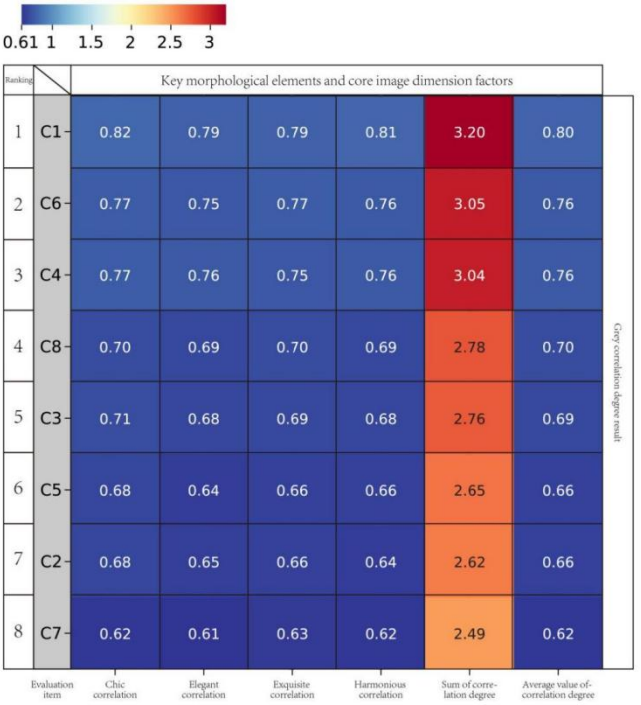


FIGURE 11. Gray Relational Averages of Morphological Elements and Imagery Factors

D. PURPLE CLAY TEAPOT GA-BPNN MAPPING MODEL CONSTRUCTION AND OPTIMIZATION

(1) BPNN MAPPING MODEL CONSTRUCTION

Using CIFs and C1, C4, C6, and C8 from Table 5, the Emotional Thinking Semantic Evaluation Matrix is used as the basic data for constructing the BPNN. The GA-BPNN model construction process is shown in Figure 12. To eliminate dimensionality differences and improve network training effectiveness, the input data are standardized according to formula (12). Taking Chic as an example, the mean and standard deviation are calculated, and the data are standardized to unify the scale, aiding neural network convergence. The BPNN structure is designed as follows: the input layer has four nodes corresponding to 4 morphological features, the hidden layer has 10 nodes, the activation function (formula 13) maps to (0, 1) and introduces nonlinearity, and the output layer has one node corresponding to the Chic prediction value, which uses the ReLU activation function. Seventy-two samples are randomly selected from the 80-sample set as the training set, and the remaining eight samples are used as the test set. The input features of the training set, X train, are a 72x4 matrix containing four morphological parameter values for 72 samples; the true Chic values of the training set, y train, are a 72x1 vector representing the Chic ratings of 72 samples. The input features of the test set, X text, are an 8x4 matrix, and the true Chic values of the test set, ytext, are an 8x1 vector. The gradient is calculated through the error, and the weights and biases are updated via gradient descent, which helps evaluate the model's generalization ability. With a maximum of 2800 iterations as the termination

condition, four BPNN models are trained, and the data for the training set are predicted. Taking Chic as an example, the trained model obtains the 72 predicted values from the training set in Table IX, reflecting the model's performance on the training set. The eight predicted values for the test set are compared with the true values to evaluate their generalizability. After training, the BPNN model's weights and biases are saved for subsequent GA optimization use.

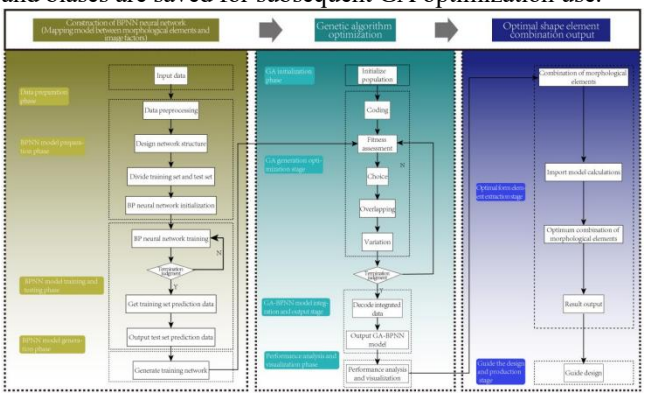


FIGURE 12. GA-BPNN Model Construction Process

TABLE IX
CHIC-GA-BPNN MODEL TRAINING SET AND TEST SET DATA

Sample	Training set	
	True value	Estimate
1	2.86	2.87
2	3.33	3.34
...	...	...
71	3.67	3.68
72	3.67	3.68
Sample	Test set	
	True value	Estimate
1	4.72	4.53
2	2.80	3.41
...	...	...
7	1.85	2.20
8	4.04	4.07

(2) GA-OPTIMIZED BPNN MAPPING MODEL

A GA is introduced to optimize the parameters of the BPNN model. A population is randomly generated, with each individual representing a set of BPNN parameters, including 40 weights from the input to the hidden layer, 11 biases in the hidden layer, and 10 weights from the hidden layer to the output layer, totaling 61 parameters encoded as real numbers to form chromosomes. The performance of the BPNN test set is used as the basis for fitness evaluation, with the mean squared error (MSE) as the fitness function (as in formula 17). The smaller the fitness value is, the better the performance of the corresponding BPNN model on the test set. On the basis of the fitness values, the roulette wheel selection method chooses superior individuals from the current population for reproduction, with each individual's selection probability (as shown in formula 18). In this way, individuals with higher fitness values are more likely to be selected, thus passing their superior genes to the next generation. Crossover operations are applied to the selected individuals to generate new individuals. The arithmetic crossover method (formula (19)) is used, which explores new parameter combinations and increases the diversity of the population. Gaussian mutation is applied to the new individuals to fine-tune the parameters, helping them escape local optima and increasing population diversity. The maximum number of iterations of 2800 is set as the termination condition. After the optimal individual is obtained, it is decoded into BPNN weights and biases and retrained to obtain the GA-BPNN model, and the weights and biases are saved for subsequent analysis.

(3) PERFORMANCE VISUALIZATION OF THE GA-BPNN MODEL

Through empirical comparison, Lv et al. (2016)[71] showed that the GA-BPNN model learns faster and more accurately than the conventional BPNN model does, with more reliable prediction results. This indicates that the predicted values in the training set are very close to the actual values, indicating good model fitting performance on the training data. The small differences between the predicted and actual values in the test set indicate strong generalizability, as shown in Figure 13. Figure 14 shows the R^2, RMSE, and MAE values for the four model groups on the training and test sets, indicating excellent fitting performance on the training data while maintaining high prediction accuracy.

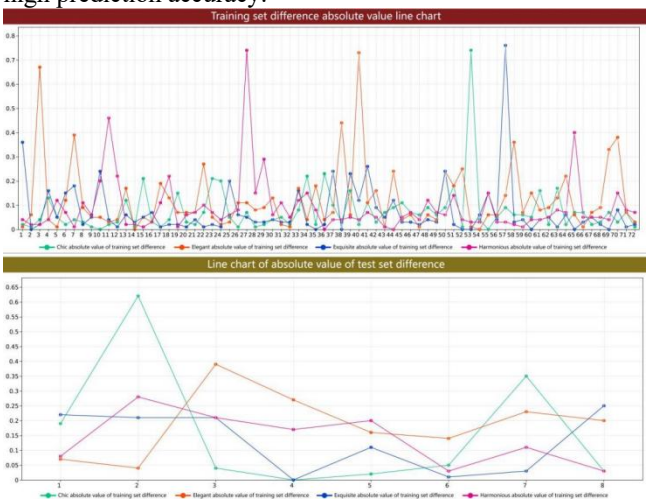


FIGURE 13. Absolute differences between training and test set predictions

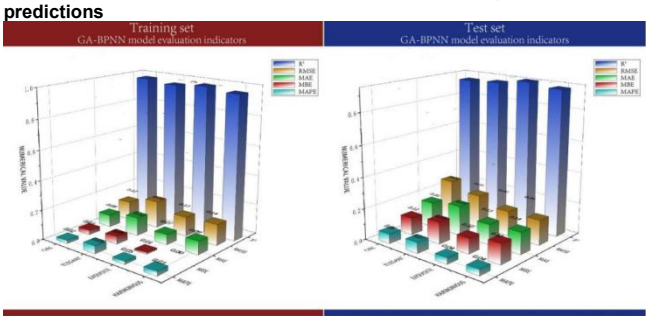


FIGURE 14. Evaluation Metrics of the GA-BPNN Model

Various visualizations are used to analyze the performance of the GA-BPNN model in predicting the imagery dimensions of purple clay teapot shapes. As shown in the two training set

plots in Figure 15, the model demonstrates good fitting and accurate predictions in the Chic and Exquisite dimensions. Although the prediction accuracy is slightly lower for the Elegant and Harmonious dimensions because of more complex shape features, the trends are still well captured.

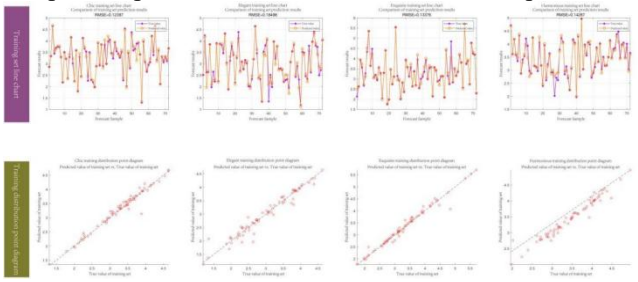


FIGURE 15. Evaluation Metrics of the GA-BPNN Model

The two test set plots in Figure 16 show that the model performs well in the Exquisite dimension. Moreover, the prediction errors are larger, and the stability is lower in the Chic and Elegant dimensions. The model's performance is weakest in the Harmonious dimension, although it still exhibits some generalizability.

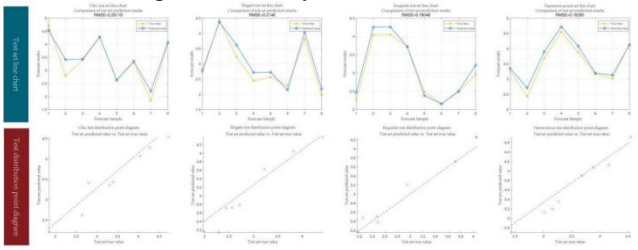


FIGURE 16. Visualization results of the GA-BPNN model on the test set

Figure 17 shows that the GA has strong search capabilities in the early stages and rapidly reduces the fitness value. Each dimension experiences local optima at different stages and durations, but ultimately, all converge successfully, improving model performance. Overall, the model shows varying performance across dimensions, providing insights for further optimization and advancing purple clay teapot shape design research.

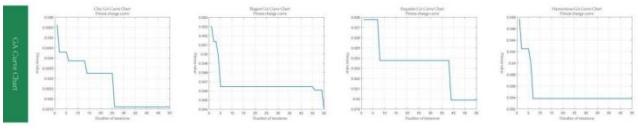


FIGURE 17. GA Curve Visualization Results

(4) OUTPUT OF OPTIMAL MORPHOLOGICAL ELEMENT COMBINATIONS

Among the top four morphological structures with the highest correlation, C1 has 14 items, C4 has three items, C6 has 10 items, and C8 has five items. Combining C1, C4, C6, and C8 into one group results in 2800 combinations, as shown in Table X. The generation of combinations can be represented by the Cartesian product of four sets, which are calculated via the following formula:

$$C1 = \{1,2 \ldots,14\},\ C4 = \{1,2 \ldots,4\},\ C6 = \{1,2 \ldots,10\},\ C8 = \{1,2 \ldots,5\} \quad (21)$$

$$Combination\ Set = C1 \times C4 \times C6 \times C8 = 14 \times 4 \times 10 \times 5 = 2800$$

TABLE X
ILLUSTRATION OF THE 2800 COMBINATIONS

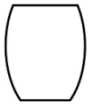
Modeling deconstruction factors (Form elements)	Form category	Combination number	C1	C4	C6	C8
Pot button (C1)	Category 1-14	1	1	1	1	1
Spout (C4)	Category 1-4	2	1	1	1	2
Pot body (C6)	Category 1-10	...	...	...	...	...
Kettle bottom (C8)	Category 1-5	2800	14	4	10	5

The 2800 processed combinations were input into the four trained GA-BPNN models to obtain predicted values across the four imagery dimensions for each combination. The average of the predicted values for each combination across the four dimensions was calculated to obtain a comprehensive score, as shown in Table XI. Ultimately, the combination with the highest comprehensive score of 4.34 was Group 1895. This group's corresponding categories of C1, C4, C6, and C8 represent the optimal morphological feature combination, as shown in Table XII optimal sample feature element column.

TABLE XI
PREDICTED VALUES FOR THE 2800 COMBINATIONS

Serial Number	Chic	Elegant	Exquisite	Harmonious	Comprehensive score
1	3.82	2.85	3.33	4.08	3.52
2	3.62	2.35	2.88	3.66	3.13
3	3.62	2.35	2.88	3.66	3.13
...	...	...	...	...	...
2798	3.41	2.83	3.33	3.22	3.20
2799	3.44	2.74	3.29	3.27	3.18
2800	3.47	2.67	3.25	3.34	3.18

TABLE XII
OPTIMAL SAMPLE FEATURE ELEMENTS

Modeling deconstruction factors (form elements)	Optimal morphology category	Schematic diagram of optimal feature elements
Pot button (C1)	Category 04 (triangle button)	
Spout (C4)	Category 04 (duck bill)	
Pot body (C6)	Category 04 (vertical oval)	
Kettle bottom (C8)	Category 04 (nailed feet)	

E. DESIGN SCHEME FOR THE PRODUCTION AND VALIDATION OF THE CLAY TEAPOT

(1) DESIGN SCHEME PRODUCTION

To verify the effectiveness of the proposed method clearly and realistically, the author used the optimal combination from Table 9 for the design study. Other design features of the purple clay teapot were selected from the highly correlated morphological elements in Figure 8. First, on the basis of the line drawing of the purple clay teapot in Figure 18, a white model and a geometric structural topology model were constructed via Rhinoceros, and three-view diagrams were generated. Then, material mapping was applied, and the model was rendered via KeyShot with ray tracing and global illumination techniques. Moreover, Cinema 4D was used to build the scene, with Octane Render handling complex materials and scene rendering. The rendered images were imported into Photoshop for color correction and Illustrator for

layout design. Finally, the usage scene of the purple clay teapot was generated, as shown in Figure 19.

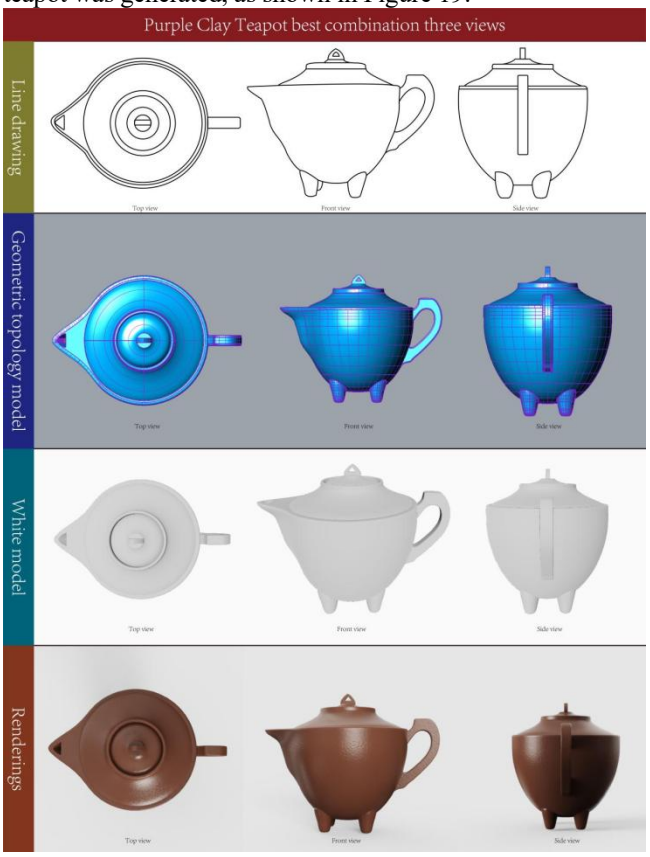


FIGURE 18. Line Drawing, White Model, Geometric Topology Model, and Rendered 3D Views

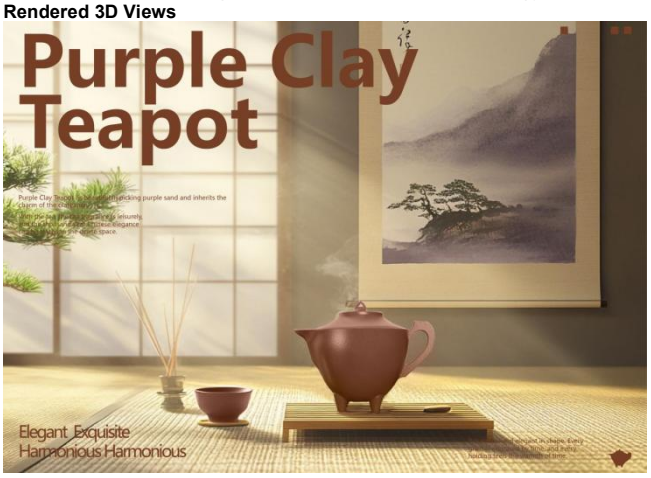




FIGURE 19. Purple Clay Teapot Usage Scene

(2) VALIDATION AND EVALUATION

To verify the feasibility of the purple clay teapot design method and its ability to meet emotional needs, a total of 308 participants were recruited, including 279 who had purchased purple clay teapots and 210 who had purchased and used them, ensuring sample representativeness and data reliability. A questionnaire was used to evaluate the design scheme, as shown in Figure 20. A 7-point Likert scale was employed, asking participants to rate four emotional imagery dimensions: “Chic,” “Elegant,” “Exquisite,” and “Harmonious.” The results showed scores of Chic (5.21), Elegant (5.3), Exquisite (5.25), and Harmonious (5.23), with an overall emotional vocabulary score of 5.25—significantly higher than the neutral midpoint score of 3.5 (see Figure 19)—indicating that the design aligns with users’ emotional needs and confirms the feasibility of the approach. Further evaluations were conducted across seven dimensions, such as the smoothness of the teapot body lines and the fit between the lid and the body. Each item had an average score above 5, with an overall average of 5.19. A total of 232 participants (75.32%) expressed satisfaction or high satisfaction. The detailed data are shown in Figures 21 and 22. Participant feedback indicated that this design method effectively meets both the functional and emotional needs of purple clay teapots, supporting future design efforts.



FIGURE 20. Multidimensional Detail Effects

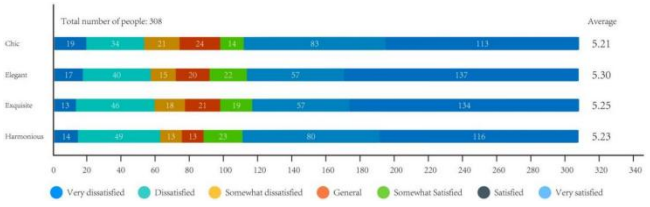


FIGURE 21. Emotional Experience Evaluation of the Shape

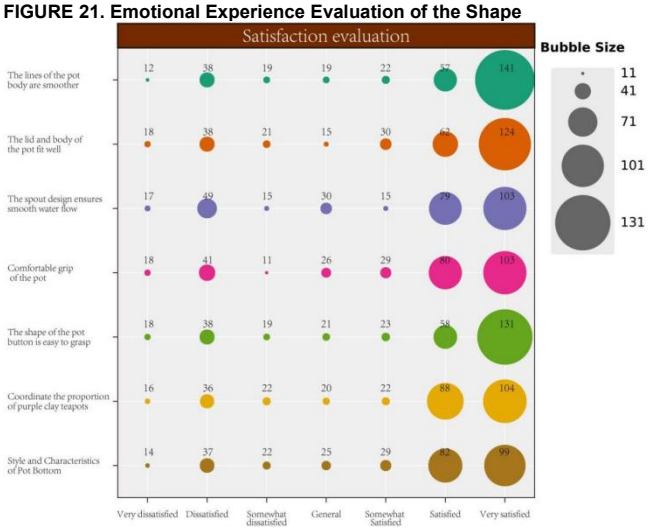


FIGURE 22. Seven-Dimensional Satisfaction Evaluation of Shape

IV. RESEARCH DISCUSSION

On the basis of KE theory, this study proposes a composite design method that integrates GRA and a GA-BPNN, which fills the gap in the quantitative analysis of purple clay teapot design and provides a replicable path for the modernization of traditional craftsmanship. The method is currently being discussed for real-world implementation with manufacturers. In prior research, Guo et al. (2019)[72] applied quality function deployment (QFD) to the iterative design of hardware tools, using the analytic hierarchy process (AHP) to rank user needs and the QFD to guide the design direction. He et al. (2021)[73] combined GRA and TOPSIS, using trapezoidal fuzzy numbers to model preferences. Xi et al. (2018)[74] applied Quantification Theory Type I to analyze user preferences. Ding et al. (2018)[75] proposed a product styling imagery evaluation method based on support vector regression (SVR). Traditional methods suffer from high subjectivity. This paper integrates FA and GRA to construct a mapping model, improving the data processing capability and addressing these issues. With advances in AI, methods such as CNNs and BPNNs are being used to convert emotional data into mathematical models for mapping product design to user sentiment. For example, Hu and Yan (2023)[76] integrated deep learning with KE theory to build a CNN model; Zhang (2024)[77] optimized the BPNN with the Kano model for ceramic products; Wang et al. (2024)[78] used a variant long short-term memory (LSTM) to predict emotion and importance; Wang et al. (2024)[79] employed a GRU-CAP model, combining gated recurrent unit (GRU) and capsule networks to enhance semantic recognition; and Le and Huh (2021)[80] used a recurrent neural network (RNN) with word vectors and CBOW architecture for sentiment classification in Vietnamese reviews. However, each approach has limitations: BPNNs tend to fall into local optima and generalize poorly; CNNs struggle with multidimensional semantic associations and risk overfitting; and RNNs, LSTMs, and GRUs are structurally complex, dependent on sequential data, and lack sufficient nonlinear representation. The proposed GA-BPNN method alleviates these issues by optimizing BPNN weights with a GA and applying dimensionality reduction via GRA, providing complementary strengths and solving three core problems. Figure 23 compares the GA-BPNN with other emotional mapping methods. Compared with traditional KE frameworks, the integrated FA/GRA/GA-BPNN approach reduces dimensionality, filters relevant features, optimizes model architecture, overcomes complexity and enables a more efficient pipeline from emotion to design.

Furthermore, interdisciplinary collaboration is expected to be a key trend. Integration with materials science (Wei and Hoi, 2022)[81], food science (Liao et al., 2018)[82], history (Jiang et al., 2022)83, and heritage studies (Zhao et al., 2023)84 will expand and enrich future research. The composite method proposed here injects innovations into purple clay teapot design and traditional craftsmanship, propelling their future development.

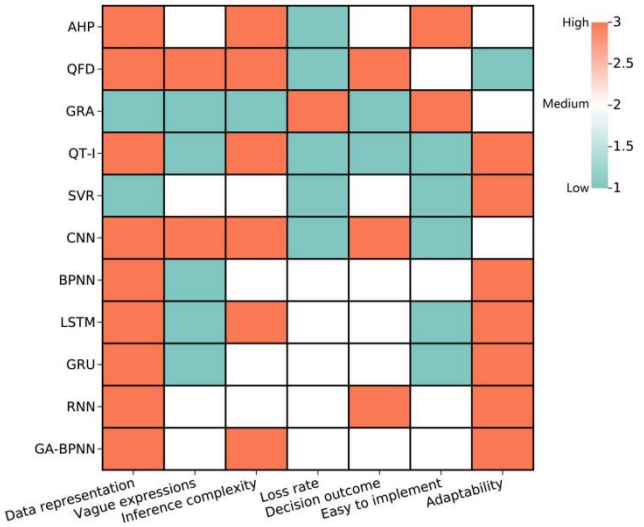


FIGURE 23. Comparison of various Kansei mapping algorithms

V. RESEARCH CONCLUSION

The main contribution of this study lies in the proposal of a composite design method based on KE, integrating GRA and the GA-BPNN to address the challenges of association and algorithmic application in purple clay teapot design. A systematic process was developed to reveal the quantitative mapping rules between purple clay teapot imagery and morphological elements, providing a data-driven foundation for design decisions. The closed-loop design process consisted of "vocabulary collection – imagery analysis – element association – model construction – design implementation – result validation." However, limitations remain: the number of samples and target users is small and lacks clear characteristics, making the results too narrow to reflect differences in consumer needs. The design verification criteria are relatively limited and lack a comprehensive evaluation that includes production feasibility and cost considerations, which hinders practical implementation. Moreover, the study lacks collaboration with materials science and manufacturing processes. This approach does not consider the evolving nature of cultural heritage, which limits the adaptability of the design methodology to future challenges.

DECLARATIONS

FUNDING

The authors declare that no funds, grants, or other financial support were received during the preparation of this manuscript.

COMPETING INTERESTS

The authors have no relevant financial or non-financial interests to disclose.

AUTHOR CONTRIBUTIONS

All authors contributed to the conception and design of the study. Material preparation, data collection, analysis, and manuscript preparation were performed collaboratively by the authors. All authors reviewed and approved the final manuscript and agreed to be accountable for the content of the work.

DATA AVAILABILITY

The datasets generated and/or analyzed during the current study are available from the corresponding author on reasonable request.

CODE AVAILABILITY

The code used for the implementation and analysis of the GA-BPNN model is available from the corresponding author on reasonable request.

ETHICS APPROVAL

The study involving human participants was conducted in accordance with the ethical principles of the Declaration of Helsinki. The requirement for formal ethical approval was waived by the Kunming University of Science and Technology Ethics Committee because the study involved an anonymous, non-interventional questionnaire-based design evaluation.

CONSENT TO PARTICIPATE

Informed consent was obtained from all participants prior to their participation in the questionnaire survey and user evaluation. Participants were informed of the purpose of the study, the voluntary nature of participation, and their right to withdraw at any time.

CLINICAL TRIAL NUMBER

Not applicable

CONSENT FOR PUBLICATION

Not applicable. The manuscript does not contain identifiable personal data, images, or other information relating to individual participants.

CONFLICT OF INTEREST

The authors declare that they have no conflict of interest.

REFERENCES

[1] 1.Young Professionals Committee & Yixing Ceramic, 2016. Decipher the science in Yixing purple-clay. Chinese Science Bulletin, 61, pp.1975–1977.

[2] 2.Chen, H.S., 2014. Analysis on the historical role and significance of purple clay teapot and its inscription decoration. In: International Conference on Education, Language, Art and Intercultural Communication (ICELAIC), 6–7 May 2014, Zhengzhou, China. Paris: Atlantis Press, pp.569–575.

[3] 3.Xian, J. & Won, L.S., 2017. A study on the characteristics of purple clay teapot in Chinese tea culture. Journal of the Korean Society of Design Culture, 23, pp.833–846.

[4] 4.Yong, S., 2010. On the artistic modeling of purple girl kettle. China's Ceramics, 46, p.63.

[5] 5.Feng, B., 2019. A study on semantic hierarchy of Zisha pot model based on Wu culture. The Eastern Art, 42, pp.333–363.

[6] 6.Zhang, J.H. & Ma, Y.Y., 2013. Manufacturing method of the purple-clay teapot mold based on reversing engineering. In: 4th International Conference on Digital Manufacturing and Automation (ICDMA), 29–30 Jun 2013, Qingdao, China. New York: IEEE, pp.760–762.

[7] 7.Fan, Z., Min, Z., Xu, H. & Cui, R., 2008. Producing technology and technique of square-shaped purple-clay teapots. China's Ceramics, 44, pp.70–71.

[8] 8.Luo, Y., 2016. Discussion on the clay features and traditional humanistic spirit of purple clay teapot. China's Ceramics, 52, pp.96–99.

[9] 9.Jie, X. & Hired, 2018. Analytical research on the decoration and manufacture techniques of Yixing purple clay teapots. The Journal of the Korean Society of Ceramic Art, 15, p.157-1.

[10] 10.Fan, Z., Min, Z. & Yang, B., 2010. Discussion on characteristic of Yixing five-color clay. China's Ceramics, 46, pp.55–58.

[11] 11.Li, X., Kim, E., Shen, Y., Zhang, X., Tu, Y. & He, P., 2021. Effect of different clay materials made boccaro teapots on Oolong tea infusion quality. *Journal of Zhejiang University. Agriculture and Life Sciences*, 47, pp.577–588.

[12] 12.Li, Y.H., Gong, G.H. & Li, N., 2018. Recent advances in modelling and optimizing complex systems based on intelligent algorithms. *International Journal of Industrial Engineering-Theory Applications and Practice*, 25, pp.779–799.

[13] 13.Mnih, V. et al., 2015. Human-level control through deep reinforcement learning. *Nature*, 518(7540), pp.529–533.

[14] 14.Gong, P.Z., Liu, J., Yang, Y.H. & He, H.H., 2020. Towards knowledge enhanced language model for machine reading comprehension. *IEEE Access*, 8, pp.224837–224851.

[15] 15.Wang, N., Li, Z., Shi, D. et al., 2024. Understanding emotional values of bionic features for educational service robots: A cross-age examination using multi-modal data. *Advanced Engineering Informatics*, 62, 102956.

[16] 16.Zhan, J.W., Meng, Y., Zhang, L.Q., Li, K.S. & Yan, F.T., 2025. Research on computer vision in intelligent damage monitoring of heritage conservation: The case of Yungang Cave Paintings. *NPJ Heritage Science*, 13.

[17] 17.Shen, J., Xu, M. & Tao, X., 2009. Reasoning mechanism of HD diagnose system based on intelligent fusion algorithm. In: *IEEE 16th International Conference on Industrial Engineering and Engineering Management*, 21–23 Oct 2009, Beijing.

[18] 18.De-Kun, J. & Memon, F.H., 2022. Design of mobile intelligent evaluation algorithm in physical education teaching. *Mobile Networks & Applications*, 27, pp.527–534.

[19] 19.Wang, N.Y., Shi, D., Li, Z.R., Chen, P.T. & Ren, X.P., 2024. Investigating emotional design of the intelligent cockpit based on visual sequence data and improved LSTM. *Advanced Engineering Informatics*, 61.

[20] 20.Zhao, K., Tao, M., Wang, M., Li, S. & Xie, L., 2013. Designing intelligent vehicle based on electromagnetic guidance. *Journal of Northwestern Polytechnical University*, 31, pp.487–490.

[21] 21.Zhou, S., Zhang, G. & Zhang, S., 2003. Application of virtual reality on concrete pump car design. *Journal of Northeastern University*, 24, pp.464–466.

[22] 22.Li, X.N. & Zhao, Z.H., 2020. Location layout design of aircraft parts assembly based on MSVR. *Chinese Journal of Aeronautics*, 33, pp.1532–1540.

[23] 23.Gong, Y.B. & Gao, Z.Y., 2024. A distributed framework for indoor product design using VR and intelligent algorithms. *International Journal of Advanced Computer Science and Applications*, 15, pp.408–417.

[24] 24.Zhou, P., 2011. The use of semantic differential method in study of sight-disabled persons' design requirements-based on the method of kansei engineering.

[25] 25.Peng, Y.H., 2008. Study of female mobile telephone design based on kansei engineering.

[26] 26.Jeong, J., 2003. Research regarding the extraction and the mutual relevancy of 'Kansei' stimulation element in sound. *Journal of Basic Design & Art*, 4, pp.100–106.

[27] 27.Uemura, S., Arisawa, H., Arikawa, M. & Kiyoki, Y., 1999. Digital media information base. *IEICE Transactions on Information and Systems*, E82D, pp.22–33.

[28] 28.Kang, X.H., Luo, Y., Zhu, Q. & Wu, C., 2025. Research on Kansei design of electric scooter integrating CNN-GRU-Attention and biologically inspired design. *Expert Systems with Applications*, 266.

[29] 29.Lai, H.H., Lin, Y.C., Yeh, C.H. & Wei, C.H., 2006. User-oriented design for the optimal combination on product design. *International Journal of Production Economics*, 100, pp.253–267.

[30] 30.Marco-Almagro, L. & Tort-Martorell, X., 2012. Statistical methods in Kansei engineering: A case of statistical engineering. *Quality and Reliability Engineering International*, 28, pp.563–573.

[31] 31.Su, J.N., Li, F.Q. & Shi, R., 2007. Research on the application of Kansei engineering. In: *International Conference on Industrial Design 2007*, 6–9 Dec 2007, Shenzhen, China. Beijing: China Machine Press, pp.86–90.

[32] 32.Bu, J., Tang, G., Sun, P. & Sha, Q., 2019. Research on ceramic teapot modeling design based on Kansei engineering. *China's Ceramics*, 55, p.67.

[33] 33.Liu, M. & IEEE, 2020. Research on modeling of palace lamps based on Kansei engineering. In: *International Conference on Intelligent Design (ICID)*, 11–13 Dec 2020, Xi'an, China. New York: IEEE, pp.257–262.

[34] 34.Wang, N. & Wang, J., 2018. Modeling design of family service robot oriented to perceptual demand. *Journal of Machine Design*, 35, pp.111–116.

[35] 35.Duan, J., Xuan, A., Yuan, B. & Li, N.N., 2022. Drawing frame modeling design based on Kansei image. *Journal of Textile Research*, 43, pp.160–166.

[36] 36.Ren, X., Wang, N., Pan, J. et al., 2025. Combining style generative adversarial networks with particle swarm optimisation-support vector regression to design affective social robot for public health intervention. *Journal of Engineering Design*, 36(1), pp.160–190.

[37] 37.Kuang, J.S. & Jiang, P.Y., 2009. Product platform design for a product family based on Kansei engineering. *Journal of Engineering Design*, 20, pp.589–607.

[38] 38.Guo, F., Qu, Q.X., Chen, P., Ding, Y. & Liu, W.L., 2016. Application of evolutionary neural networks on optimization design of mobile phone based on user's emotional needs. *Human Factors and Ergonomics in Manufacturing & Service Industries*, 26, pp.301–315.

[39] 39.Zhang, S.X., Lv, G.L., Guo, S.F., Zhang, Y.H. & Feng, W., 2021. Porosity characterization of thermal barrier coatings by ultrasound with genetic algorithm backpropagation neural network. *Complexity*, 2021.

[40] 40.Sun, B., Zheng, W., Tong, A., Di, D.Y. & Li, Z.W., 2023. Prediction of the roughness coefficient for drainage pipelines with sediments using GA-BPNN. *Water Science and Technology*, 88, pp.1111–1130.

[41] 41.Hu, H.F. & He, W.N., 2016. Research on key technology of network intrusion detection system based on improved GA-BPNN algorithm. In: *3rd International Conference on Applied Engineering*, 22–25 Apr 2016, Wuhan, China, p.391.

[42] 42.Young, O.S. & Hong, H.J., 2007. Combination of research methods for factor analysis. *The Journal of the Korea Contents Association*, 7, pp.202–210.

[43] 43.Liu, Y., Zhu, Q., Lv, L., Liao, K. & Xu, F., 2016. Optimizing soil moisture monitoring based on temporal stability and factor analysis. *Soils*, 48, pp.186–192.

[44] 44.Mainous, A.G., 3rd, 1993. Factor analysis as a tool in primary care research. *Family Practice*, 10, pp.330–336.

[45] 45.Silver, H. & Hyung-Ryong, L., 2013. Importance-performance analysis of educational service. *Journal of Tourism and Leisure Research*, 25, pp.479–498.

[46] 46.YU, S. & LIU, Z. 2022. Risk consensus assessment of credit suppliers based on the FA-KM-GAHP model. Journal of Shanghai University. Natural Science Edition, 28, 1008-1021.

[47] 47.Chen, H., Shi, L. & Wang, Z., 2021. Interior design of offshore platform accommodation cabin based on kansei image. *Journal of Machine Design*, 38, pp.139–144.

[48] 48.Jing, Y., Cheng, Y.S., Yu, S. & Lin, J.Y., 2024. An innovative application of diagonal ridge elements of classical Suzhou-style buildings to furniture design based on Kansei engineering and shape grammar. *Bioresources*, 19, pp.5549–5567.

[49] 49.Su, K., Sun, S., Chai, C., Sun, L. & Liu, Z., 2011. Customized product material image decision-making support model. *China Mechanical Engineering*, 22, pp.1723–1728.

[50] 50.Xie, M. & Chen, X., 2019. Advances in the application of bibliometrics-based grey system theory in fisheries science. *Transactions of Oceanology and Limnology*, pp.117–126.

[51] 51.Fujun, Y.I., Wei, D., Xi, C. & Bai, C.A.O., 2010. Research on adaptability evaluation for road network in economic circle. *Journal of Highway and Transportation Research and Development*, 27, pp.144–148.

[52] 52.YANG, X. Y., WANG, S. C., PENG, Y., CHEN, J. W. & MENG, L. Z. C. 2023. Short-term photovoltaic power prediction with similar-day integrated by BP-AdaBoost based on the Grey-Markov model. Electric Power Systems Research, 215.
[53] 53.Li, J., Ren, S. & Li, Y., 2018. Comprehensive evaluation of regional higher education development based on data analysis. *Science & Technology for Development*, 14, pp.534–540.
[54] 54.Dong, G.F., Wei, W., Xia, X., Wozniak, M. & Damaševicius, R., 2020. Safety risk assessment of a Pb-Zn mine based on fuzzy-grey correlation analysis. *Electronics*, 9.
[55] 55.Xu, J., Wang, X., Huang, P., Wang, Y. & Chu, Y., 2016. Research on prediction methods of automobile styling based on the grey correlation theory. *Journal of Machine Design*, 33, pp.114–117.
[56] 56.Zhang, S., Zhang, F., Wang, Y., Yang, Z., Liu, Y. & Li, C., 2023. Modeling design of construction hoist based on shape grammar and grey correlation. *Journal of Machine Design*, 40, pp.157–163.
[57] 57.Xue, L. & Yi, X., 2019. Research on modeling and color design of high-speed train seat image. *Journal of Machine Design*, 36, pp.139–144.
[58] 58.Du, G.S., Liu, Z.X. & Lu, H.F., 2021. Application of innovative risk early warning mode under big data technology in internet credit financial risk assessment. *Journal of Computational and Applied Mathematics*, 386.
[59] 59.Liu, Y.P., Wu, M.G. & Qian, J.X., 2006. Evolving neural networks using the hybrid of ant colony optimization and BP algorithms. In: Wang, J., Yi, Z., Zurada, J.M., Lu, B.L. & Yin, H.J. (eds.) *Advances in Neural Networks – ISNN 2006, Pt 1*.
[60] 60.Sun, W.J., Zhao, R., Yan, R.Q., Shao, S.Y. & Chen, X.F., 2017. Convolutional discriminative feature learning for induction motor fault diagnosis. *IEEE Transactions on Industrial Informatics*, 13, pp.1350–1359.
[61] 61.Sang, B., 2021. Application of genetic algorithm and BP neural network in supply chain finance under information sharing. *Journal of Computational and Applied Mathematics*, 384.
[62] 62.Ding, M., Ding, T., Song, M., Zhang, X. & Liu, Z., 2023. Product color emotional design method based on implicit measurement and BP neural network. *Computer Integrated Manufacturing Systems*, 29, pp.616–627.
[63] 63.Guo, F., Liu, W.L., Cao, Y.Q., Liu, F.T. & Li, M.L., 2016. Optimization design of a webpage based on Kansei engineering. *Human Factors and Ergonomics in Manufacturing & Service Industries*, 26, pp.110–126.
[64] 64.Museum, W., Lee, J. & Daewon Kim, 2015. Effective robot path planning method based on fast convergence genetic algorithm. *Journal of The Korea Society of Computer and Information*, 20, pp.25–32.
[65] 65.Azuma, R., Sakamoto, M. & Furutani, H., 2009. Haplotype estimation from genotypical data by genetic algorithm. *Artificial Life and Robotics*, 13, pp.535–537.
[66] 66.Shi, X.H., 2020. Research on the optimisation of complex models of large-scale building structures dependent on adaptive grey genetic algorithms. *International Journal of Biometrics*, 12, pp.13–28.
[67] 67.Son, L.D., An, T.V. & Thuy, N.N., 2021. Improving the asymmetric encryption algorithm based on genetic algorithm, application in online information transmission. *International Journal of Electronic Security and Digital Forensics*.
[68] 68.Yu, J., 2008. Studies on genetic algorithm in image restoration application.
[69] 69.Diego-Mas, J.A., Poveda-Bautista, R. & Alcaide-Marzal, J., 2016. Designing the appearance of environmentally sustainable products. *Journal of Cleaner Production*, 135, pp.784–793.
[70] 70.Tian, G.F., 2008. Research on theory of artificial neural networks and its application in automobile designing.
[71] 71.Lv, W., Wang, M. & Zhu, X., 2016. Model for prediction of surface subsidence coefficient in backfilled coal mining areas based on genetic algorithm and BP neural network. *Journal of Computational Methods in Sciences and Engineering*, 16(4), pp.745–753.
[72] 72.Guo, X., Nie, X. & Wang, J., 2019. Research of hardware tools design based on QFD. *Journal of Machine Design*, 36, pp.122–126.
[73] 73.He, J., Chen, D. & Yu, S., 2021. Multi-cultural image color design evaluation methods for creative products of tourism culture. *Mechanical Science and Technology for Aerospace Engineering*, 40, pp.92–100.
[74] 74.Xi, L., Wu, Y., Ye, J., Xiao, W. & Cheng, J., 2018. Modelling design of mini electric vehicle based on attractive factors. *Journal of Graphics*, 39, pp.661–667.
[75] 75.Ding, M., Xu, F., Zhao, F. & Liu, R., 2018. Product modeling image evaluation method based on evolutionary law and support vector regression. *Journal of Machine Design*, 35, pp.105–110.
[76] 76.Hu, Y. & Yan, K., 2023. Convolutional neural network models combined with Kansei engineering in product design. *Computational Intelligence and Neuroscience*, 2023, 2572071.
[77] 77.Zhang, Y.L., 2024. Daily ceramic product design method based on optimized BP neural network model and Kano model. *Journal of Ceramic Science and Technology*, 15, pp.7–20.
[78] 78.Wang, K., Wang, Z., Li, J. & Tong, S., 2024. Customer preference analysis and prediction for product design improvement. *Computer Integrated Manufacturing Systems*, 30, pp.1989–2004.
[79] 79.Wang, Z., Hu, S.J. & Liu, W.D., 2024. Product feature sentiment analysis based on GRU-CAP considering Chinese sarcasm recognition. *Expert Systems with Applications*, 241.
[80] 80.Le, N.B.V. & Huh, J.H., 2021. Applying sentiment product reviews and visualization for BI systems in Vietnamese e-commerce website: Focusing on Vietnamese context. *Electronics*, 10.
[81] 81.Wei, Z. & Choi, S., 2022. A comparative study of Jeju clay and Yixing clay. *The Journal of the Korean Society of Ceramic Art*, 19, pp.67–80.
[82] 82.Liao, Z.H., Chen, Y.J., Tzen, J.T.C., Kuo, P.C., Lee, M.R., Mai, F.D., Rairat, T. & Chou, C.C., 2018. Effect of teapot materials on the chemical composition of oolong tea infusions. *Journal of the Science*.
[83] 83.Jiang, G., Pan, S. & Yu, T., 2022. Evolution of patterns between Zisha-stoneware exported in the Ming and Qing dynasty and European imitations. *China's Ceramics*, 58, pp.98–106.
[84] 84.Zhao, M., Zhai, Y., Zhao, J., Zhou, W.H., Zhao, L., Ge, Y., Zhang, K.X. & Luo, H.J., 2023. Microbial corrosion on underwater pottery relics with typical biological condensation disease. *Heritage Science*, 11.29, no. 4, pp. 439–448, Sep. 2011.